Purification, Bioactivity, and Secondary Structure Analysis of Mouse and Human Macrophage Migration Inhibitory Factor (MIF)†

Jürgen Bernhagen,‡,§ Robert A. Mitchell,‡ Thierry Calandra,‡ Wolfgang Voelter,§ Anthony Cerami,‡ and Richard Bucala*,‡

The Picower Institute for Medical Research, 350 Community Drive, Manhasset, New York 11030, and Abteilung für Physikalische Biochemie, Physiologisch-chemisches Institut der Universität Tübingen, Hoppe-Seyler Strasse 4, D-72076 Tübingen, Germany

Received April 7, 1994; Revised Manuscript Received September 6, 1994⊗

ABSTRACT: The cytokine macrophage migration inhibitory factor (MIF) has been identified to be secreted by the pituitary gland and the monocyte/macrophage and to play an important role in endotoxic shock. Despite the recent molecular cloning of a human T-cell MIF, characterization of the biochemical and biological properties of this protein has remained incomplete because substantial quantities of purified, recombinant, or native MIF have not been available. We describe the cloning of mouse MIF from anterior pituitary cells (AtT-20) and the purification of native MIF from mouse liver by sequential ion exchange and reverse-phase chromatography. For comparison purposes, human MIF was cloned from the Jurkat T-cell line and also characterized. Mouse and human MIF were highly homologous (90% identity over 115 amino acids). Recombinant mouse and human MIF were expressed in *Escherichia coli* and purified in milligram quantities by a simple two-step procedure. The molecular weight of native mouse MIF (12.5 kDa monomer) was identical with that of recombinant mouse MIF as assessed by gel electrophoresis and mass spectroscopy. No significant post-translational modifications were detected despite the presence of two potential N-linked glycosylation sites. Recombinant MIF inhibited monocyte migration in a dose-dependent fashion, and both recombinant and native MIF exhibited comparable biological activities. MIF induced the secretion of tumor necrosis factor-α and stimulated nitric oxide production by macrophages primed with interferon-γ. Circular dichroism spectroscopy revealed that bioactive mouse and human MIF exhibit a highly ordered, three-dimensional structure with a significant percentage of β-sheet and α-helix conformation. Guanidine hydrochloride-induced unfolding experiments demonstrated that MIF is of low to moderate thermodynamic stability. These studies establish the biochemical identity of native and recombinant MIF and provide a first insight into the three-dimensional structural properties of this critical inflammatory mediator.

The cytokine macrophage migration inhibitory factor (MIF)[1] was described originally as a T-lymphocyte-associated activity which inhibited the random migration of guinea pig peritoneal macrophages (Bloom & Bennett, 1966; David, 1966). Over the years, MIF activity has been reported to be associated with delayed-type hypersensitivity (Bloom & Bennett, 1966; David, 1966), to be produced by lectin-activated T-cells (Weiser *et al.*, 1981), and to enhance macrophage adherence, phagocytosis (Nathan *et al.*, 1971, 1973), and tumoricidal activity (Churchill *et al.*, 1975; Pozzi & Weiser, 1992). We recently identified the mouse homolog of MIF to be a novel protein released by the anterior pituitary gland in response to endotoxin (LPS) administration. Pituitary MIF was found to contribute to circulating MIF levels during shock, and exogenous MIF increased markedly the lethality of experimental endotoxemia in mice (Bernhagen *et al.*, 1993). Subsequent studies also have identified MIF to be produced by activated macrophages, suggesting that these cells are not only an important target but also an important source of MIF protein *in vivo* (Calandra *et al.*, 1994).

A number of the biological activities attributed to MIF over the years have remained ambiguous since many studies were performed with lymphocyte-conditioned medium which was subsequently shown to contain other cytokines with MIF activity, such as interferon-γ (IFN-γ) and interleukin-4 (IL-4) (McInnes & Rennick, 1988; Thurman *et al.*, 1985). Despite the recent cloning of a human T-cell MIF (Weiser *et al.*, 1989), significant quantities of purified, bioactive material have not been available, thus hampering characterization of the precise biochemical and biological properties of this protein. Furthermore, recombinant human MIF prepared from a eukaryotic COS cell expression system

† Supported by the National Institutes of Health (AI21359), the Arthritis Foundation, a grant from the Fonds de perfectionnement du Centre Hopitalier Universitaire Vaudois, Lausanne, Switzerland, and the Swiss Foundation for Research in Medicine and Biology.

* To whom correspondence should be addressed.

‡ The Picower Institute for Medical Research.

§ Physiologisch-chemisches Institut der Universität Tübingen.

⊗ Abstract published in *Advance ACS Abstracts,* November 1, 1994.

[1] Abbreviations: MIF, macrophage migration inhibitory factor; rmuMIF, recombinant mouse MIF; rhuMIF, recombinant human MIF; TNF-α, tumor necrosis factor-α; IL, interleukin; LPS, lipopolysaccharide; IFN-γ, interferon-γ; GIF, glycosylation inhibiting factor; GST, glutathione-*S*-transferase; CD, circular dichroism; θ, mean residue molar ellipticity; GdnHCl, guanidine hydrochloride; TFE, 2,2,2-trifluoroethanol; DTT, dithiothreitol; Tris, tris(hydroxymethyl)aminomethane; NO, nitric oxide; FPLC, fast protein liquid chromatography; RP, reverse-phase; RT/PCR, reverse transcription/polymerase chain reaction; IPTG, isopropyl 1-thio-β-D-galactopyranoside; CAPS, 3-(cyclohexylamino)-1-propanesulfonic acid; M_r, relative molecular weight; SDS−PAGE, sodium dodecyl sulfate−polyacrylamide gel electrophoresis.

0006-2960/94/0433-14144$04.50/0

recently has been shown to contain a mitogenic contaminant (David, 1993a,b).

In the present report, we describe the cloning of mouse MIF (muMIF) from an anterior pituitary cell line and the purification of native MIF from mouse liver. For comparison purposes, we also cloned human MIF (huMIF) from the Jurkat T-cell line. Recombinant mouse and human MIF were expressed in *Escherichia coli* and purified to homogeneity by a simple two-step procedure, and the proteins were characterized by a variety of biochemical and biological criteria. In addition, circular dichroism (CD) spectroscopy and thermodynamic stability studies were performed to obtain information concerning the three-dimensional structure of this protein.

EXPERIMENTAL PROCEDURES

Materials. Polymerase chain reaction (PCR), reverse transcription (RT), and other molecular biology reagents were purchased from Gibco BRL (Grand Island, NY) unless stated otherwise. PCR buffer was from Perkin Elmer Cetus (Norwalk, CT), RNAse inhibitor "RNAsin" was obtained from Promega (Madison, WI), RNAzol B was from TEL-TEST, Inc. (Friendswood, TX), and oligonucleotides were purchased from OLIGOS ETC., Inc. (Wilsonville, OR). Manual DNA sequencing was performed with the SEQUENASE 2.0 system (United States Biochemical, Cleveland, OH; Tabor & Richardson, 1987). For automated DNA sequencing, the *Taq* DyeDeoxy Terminator Cycle Sequencing Kit (Applied Biosystems Inc., Foster City, CA) was utilized. Western blotting was performed following a modification of the method by Anderson *et al.* (1982). Sodium dodecyl sulfate−polyacrylamide gel electrophoresis (SDS−PAGE) and Western blotting reagents were from Pierce (Rockford, IL). Polyclonal anti-rmuMIF antiserum was prepared from rabbits immunized with purified rmuMIF as described elsewhere (Bernhagen *et al.*, 1993). Thioglycollate broth (Difco, Detroit, MI) was prepared according to the manufacturer's recommendation, autoclaved, and stored protected from light at room temperature. *E. coli* O111:B4 LPS and polymyxin B were purchased from Sigma (St. Louis, MO). LPS was resuspended in pyrogen-free water, vortexed, sonicated, aliquoted (5 mg/mL), and stored at −20 °C. Serial dilutions of LPS were prepared in pyrogen-free water and sonicated (Branson 3210, Danbury, CT) for 10 min prior to use.

Cloning of Mouse and Human MIF. Mouse MIF was cloned from the mouse anterior pituitary cell line AtT-20/D16v-F2 (American Type Culture Collection, Rockville, MD). Cells were plated at 1×10^6 cells/mL in DMEM containing 50 μg/mL gentamicin (Gibco BRL) and 10% heat-inactivated fetal bovine serum (FBS) (HyClone, Logan, UT). After 3 h of incubation at 37 °C in a humidified atmosphere with 5% CO_2, nonadherent cells were removed and the remaining adherent cells washed twice with DMEM/10% FBS. LPS (50 μg/mL) then was added, and the cells were incubated for 16 h. At the end of this time, cell culture medium was removed and total RNA was isolated with RNAzol B according to the manufacturer's instructions. One microgram of RNA was reverse transcribed using $(dT)_{12-18}$ and M-MLV reverse transcriptase in a 50 μL reaction. Five microliters of cDNA was amplified by PCR (32 cycles; 1 min at 94 °C, 1 min at 55 °C, 1 min at 72 °C) using MIF primers described previously (Bernhagen *et al.*, 1993). A single DNA amplification product of expected size was obtained and purified using the GENE CLEAN II Kit (BIO 101 Inc., La Jolla, CA). The cDNA then was cloned into the plasmid pT7Blue and transformed into Nova Blue competent *E. coli* using the pT7Blue T-Vector Kit (Clark, 1988; Novagen, Madison, WI). Recombinant DNA was prepared from multiple white colonies using the Plasmid Magic Minipreps DNA Purification System (Promega) and sequenced manually in a Sequi-Gen II Sequencing Cell (Bio-RAD, Hercules, CA). The mouse AtT-20 MIF cDNA sequence is entered in the EMBL Data Bank under accession number Z23048.

For huMIF cloning, Jurkat H33HJ-JA1 cells (American Type Culture Collection) were plated at 1×10^6 cells/mL in RPMI containing 50 μg/mL gentamicin and 10% heat-inactivated FBS. After 3 h of incubation at 37 °C in a humidified atmosphere with 5% CO_2, nonadherent cells were removed and the remaining adherent cells washed twice with RPMI/10% FBS. Cells were incubated for another hour, and the total RNA was isolated and subjected to RT as described above. *Nde*I/MIF and *Bam*HI/MIF fusion primers (5′-CCATATGCCGATGTTCATCGTAAACAC-3′ and 3′-CGGATCCTGCGGCTCTTAGGCGAAGG-5′) were designed from a huMIF cDNA sequence (Weiser *et al.*, 1989) and used to amplify huMIF cDNA as described above. A single PCR product of predicted size was obtained, purified using the GENE CLEAN II Kit, and ligated into the *Nde*I/*Bam*HI-digested pET11b vector (Novagen). *E. coli* DH5α was transformed with the ligation mixture, and the single recombinant colonies were isolated after overnight growth. Plasmid DNA was prepared from eight clones and the MIF insert sequenced bidirectionally by automated methods using an ABI Model 373A DNA sequencer (Applied Biosystems Inc.). The human Jurkat H33HJ-JA1 MIF cDNA sequence is entered in the EMBL Data Bank under accession number Z23063.

Expression and Purification of Recombinant MIF. The recombinant pT7Blue clone containing muMIF cDNA was digested with the restriction enzymes *Nde*I and *Bam*HI, and the MIF insert was isolated and ligated into the *Nde*I/*Bam*HI-digested pET11b vector (Studier *et al.*, 1990; Novagen). *E. coli* DH5α was transformed, and the single recombinant colonies were isolated and stored in 20% glycerol at −80 °C until use. Mouse or human MIF-containing pET11b plasmid DNA then was prepared and used to transform the *E. coli* BL21(DE3) expression strain (Novagen). One liter cultures were grown at 37 °C until the optical density at 600 nm reached 0.6−0.8. Isopropyl 1-thio-β-D-galactopyranoside (IPTG) was added to a final concentration of 1 mM and the incubation continued at 37 °C for an additional 3 h. Bacteria then were harvested by centrifugation and the cell pellets frozen at −20 °C until use. For protein purification, the bacterial pellets (corresponding to 50 mL of culture) were thawed and resuspended in 3.5 mL of Tris-buffered saline (50 mM Tris-HCl, 150 mM NaCl, pH 7.5). The bacteria were lysed by adding an equal volume of washed glass beads (106 μm; Sigma, G-8893) and vortexing the mixture vigorously for 10 min. Lysis was confirmed by examination under phase contrast microscopy. Glass beads were removed by centrifugation at 1000*g* for 10 min, and the bacterial extract then was centrifuged at 38000*g* for 30 min. The supernatant,

representing the cleared bacterial lysate, was sterile-filtered through a 45 μm and then a 22 μm membrane filter and subjected to MONO Q anion exchange chromatography using a fast protein liquid chromatography system (FPLC) (Pharmacia, Piscataway, NJ). The Mono Q column was equilibrated with Tris-buffered saline. MIF was eluted with the same buffer in the first flow-through fractions (3 mL), which were pooled and placed on ice immediately. The MIF-containing fractions then were applied to a C8-SepPak reverse-phase (RP) column (Waters, Division of MILLIPORE, Milford, MA) that had been washed first with methanol followed by water. Unbound material was eluted by washing the resin with 10 column volumes of water and 20% acetonitrile/water, respectively. MIF then was eluted with six column volumes of 60% acetonitrile/water, frozen at −80 °C, lyophilized, and kept at −20 °C until use. For renaturation, MIF was dissolved at a concentration of 200−400 μg/mL in 20 mM sodium phosphate buffer (pH 7.2) containing 8 M urea and 5 mM DTT and dialyzed against 20 mM sodium phosphate buffer (pH 7.2) containing 5 mM DTT followed by 20 mM sodium phosphate buffer (pH 7.2) alone. Renatured MIF was sterile-filtered and kept at 4 °C until use. The LPS content of MIF preparations was determined by the chromogenic *Limulus* amoebocyte assay (Bio-Whittaker Inc., Walkersville, MD). Attempts to purify rmuMIF from the cleared bacterial lysate by affinity chromatography with *S*-hexylglutathione−agarose beads (Sigma, H-7011) were performed following the method for single-step purification of protein/glutathione-*S*-transferase fusion constructs (Smith & Johnson, 1988).

Purification of Native MIF. Two grams of mouse liver acetone powder (Sigma, L-8254) were resuspended in 20 mL of Tris-buffered saline and vortexed, and the insoluble material was removed by centrifugation at 1000*g* for 10 min. The supernatant, containing MIF and other hepatic proteins, was filtered (a 45 μm followed by a 22 μm filter) and subjected to MONO Q/FPLC anion exchange chromatography as described above. MIF eluted with the first flow-through fractions (3 mL), which were pooled and applied to a Pro S cation exchange column (kindly donated by BIO-RAD) that was equilibrated with Tris-buffered saline. MIF eluted with Tris-buffered saline, and the MIF-containing fractions again were recovered from the flow-through. The MIF fractions then were pooled and applied to a C8-SepPak cartridge. MIF was eluted with 60% acetonitrile/water, lyophilized, and stored as described above. Attempts to purify liver MIF from mouse liver supernatant by affinity chromatography with *S*-hexylglutathione−agarose beads were performed as described above.

Biochemical Characterization of MIF. SDS−PAGE was performed in 18% gels under reducing conditions (Laemmli, 1970). The gels were either stained with silver or processed further for Western blotting. For silver staining, gels first were fixed for 16 h in 50% methanol/10% acetic acid and then analyzed as described (Poehling & Neuhoff, 1981). For Western blotting, proteins were transferred to nitrocellulose membrane (Schleicher & Schuell, Keene, NH) by electroblotting at 50 V and 150 mA for 16 h using CAPS transfer buffer (10 mM CAPS, 20% methanol, pH 11.0). Membranes then were incubated with blocking buffer (50 mM Tris-HCl, 500 mM NaCl, pH 7.5, 5% nonfat dry milk, 0.05% Tween-20) followed by incubation with a 1:1000 dilution of polyclonal rabbit anti-rmuMIF antiserum in binding buffer (50 mM Tris-HCl, 500 mM NaCl, pH 7.5, 1% BSA, 0.05% Tween-20). After extensive washing in binding buffer, membranes were incubated with a 1:1000 dilution of horseradish peroxidase-conjugated goat antirabbit antibody (Pierce) in binding buffer, washed twice with binding buffer and twice with 50 mM Tris-base (pH 7.5) containing 150 mM NaCl, and developed with chloronaphthol/H_2O_2 substrate. Prestained protein molecular weight (M_r) markers ranged from 2.5 to 43 kDa (Gibco BRL).

N-terminal MIF sequence was determined by Edman degradation (Allen, 1981) and automated gas-phase sequencing following a manufacturer's protocol (Applied Biosystems).

For N-glycosylation analysis, 0.1 μg of purified liver-derived MIF was incubated with the endoglycosidase PNGase F according to the manufacturer's instructions (New England BioLabs, Beverly, MA). Samples then were mixed 1:1 with Laemmli electrophoresis buffer and boiled for 5 min, and one-fourth of the incubation mixture was analyzed by SDS−PAGE/Western blotting as described above. To control for digestion efficiency, IgG light and heavy chains were digested in parallel and resolved on the same gel. Digestion was assessed to be complete after 3 h of incubation with 5000 units/mL PNGase F.

For analytical size exclusion chromatography, 40 μg of purified rmuMIF or rhuMIF was dissolved in 200 μL of 20 mM sodium phosphate buffer (pH 7.2) containing 7 M GdnHCl. The sample was separated over a Superose 12 HR 10/30 column (Pharmacia), equilibrated with the same buffer, and eluted at a flow rate of 0.5 mL/min. Size markers were from BIO-RAD (1.35−670 kDa) and were chromatographed under the same conditions.

Mass spectrometric analysis (MS) of MIF was performed by matrix-assisted laser desorption ionization MS as described elsewhere (Hillenkamp & Karas, 1990) using a Shimadzu Kratos Kompact MALDI 3 V3.0.2 machine (Hannover, Germany). Twenty individual spectra were accumulated for each mass analysis. In addition, rmuMIF was analyzed by ion-spray mass spectroscopy (IS-MS) using an API III triple quadrupole mass spectrometer with an IonSpray interface (Sciex, Toronto).

Purified, renatured rmuMIF (20 μg/mL) and MIF-containing bacterial lysates (estimated MIF content, 50 μg/mL) were analyzed photometrically for glutathione-*S*-transferase (GST) activity by the method of Fjellstedt *et al.* (1973) using 1,2-epoxy-3-(*p*-nitrophenoxy)propane (EPNP) as a substrate and bovine GST (Sigma, G-8386) as a positive control (Blocki *et al.*, 1992). In this assay system, bovine GST (400 μg/mL) was found to have an enzyme activity of 0.014 unit/mL with respect to the substrate EPNP.

Bioactivity Profile. The macrophage/monocyte migration inhibitory activity of recombinant MIF was analyzed by studying the migration of human peripheral blood monocytes in modified Boyden chambers (Boyden, 1962). Monocytes were isolated from heparinized venous blood of healthy donors (Timonen & Saksela, 1980) and resuspended at a concentration of 2.5×10^6 cells/mL in Gey's balanced salts solution (Gibco BRL) containing 2% fatty acid-free bovine serum albumin (Sigma) and 20 mM Hepes (pH 7.2). MIF-containing (0.0001-10 μg/mL) solutions or buffer controls were placed in the lower compartment of the Boyden chamber and covered tightly by a poly(vinylpyrrolidone)-free polycarbonate filter (5 μm pore size; no. 155845, Costar

Corp., Cambridge, MA) and monocytes (1×10^5) added to the compartment above the filter. The chambers then were incubated for 3 h at 37 °C in a humidified atmosphere with 5% CO_2. At the end of this time, the filters were recovered and the cells fixed and stained with Giemsa reagent. Monocytes then were counted as described previously (Sherry *et al.*, 1992).

Tumor necrosis factor-α (TNF-α) production was quantitated in MIF-conditioned RAW 264.7 macrophage supernatants by L929 cell cytotoxicity as described previously (Wolpe *et al.*, 1988). RAW 264.7 macrophages were resuspended in RPMI/10% FBS, plated at 1×10^6 cells/mL, incubated for 3 h at 37 °C in a humidified atmosphere with 5% CO_2, and washed twice with RPMI/1% FBS. Cells were incubated for 12−14 h with various doses at MIF diluted in RPMI/1% FBS. At the end of each experiment, cell culture media were collected, centrifuged (10 min at 800*g*), and supplemented with 1 mM PMSF. MIF-induced TNF-α activity was measured immediately afterwards. Polyclonal rabbit anti-recombinant mouse TNF-α antiserum (50 μL/mL) blocked TNF activity completely, and MIF did not contribute to TNF-α activity as recombinant mouse TNF-α (rTNF-α) (5 pg/mL−1 μg/mL) cytotoxicity remained unchanged when rmuMIF (10 pg/mL−10 μg/mL) or anti-rmuMIF antibody was added to L929 cells together with rTNF-α.

Nitric oxide (NO) production was quantitated in MIF-conditioned RAW 264.7 and thioglycollate-elicited peritoneal exudate macrophage supernatants by measuring nitrite and nitrate content with the Griess reagent (Stuehr & Marletta, 1987). RAW 264.7 macrophages were prepared and conditioned as described above. In some experiments, cells were incubated for 1 h with recombinant mouse interferon-γ (IFN-γ) (100 IU/mL) (Boehringer-Mannheim, Indianapolis, IN) prior to the addition of MIF. Thioglycollate-elicited peritoneal exudate macrophages were obtained from BALB/c mice that were injected intraperitoneally 3−4 days previously with 2 mL of sterile thioglycollate broth. Cells were harvested under strict aseptic conditions by lavage of the peritoneal cavity with 5 mL of an ice-chilled 11.6% sucrose solution. After centrifugation (10 min at 800*g*), cells were resuspended in RPMI/10% FBS and plated at a density of 2×10^6 cells/mL. After 3 h of incubation, nonadherent cells (*i.e.*, PMNs, lymphocytes) were removed with RPMI/1% FBS and the remaining adherent cells conditioned with MIF as described for RAW 264.7 cells. LPS traces were neutralized by incubating MIF (1 and 10 μg/mL in cell culture media) with polymyxin B at a concentration of 10 and 100 ng/mL, respectively, for 30 min at room temperature under sterile conditions. The mixture was cleared by centrifugation and added to the prepared macrophage cultures. The polymyxin B concentration added was approximately 1000-fold higher than necessary to neutralize the contaminating LPS present (Calandra *et al.*, 1994). For antibody neutralization of MIF activity, rmuMIF (1 and 10 μg/mL in cell culture media) was treated with 20 μL/mL anti-rmuMIF or normal rabbit control serum and added to the macrophages as described above.

Conformational and Structural Stability Analysis. CD spectra were recorded on an Aviv Associates Model 62DS spectropolarimeter. The spectra represent the average of three scans recorded at 25 °C in the range between 190 and 250 nm and were collected at 0.25 nm intervals, with a band width of 1.5 nm and a time constant of 1.0 s. The quartz cells (1 and 10 mm) used in all CD measurements were washed with 30% HCl in ethanol, rinsed with water and methanol, and dried before use. Protein concentrations were determined from stock solutions prepared in 20 μM phosphate buffer (pH 7.2) using the Bio-Rad protein assay (BIO-RAD) Bradford, 1976). This assay was found to agree with values obtained by quantitative amino acid analysis. Thirty minutes before CD analysis, proteins were diluted from the stock solutions to a final concentration of 10 μM in 20 mM phosphate buffer (pH 7.2), unless stated otherwise. CD spectra are presented as a plot of the mean molar ellipticity per residue ($[\theta]$, deg cm^2 dmol^{-1}) versus the wavelength.

For unfolding experiments, MIF stock solutions dissolved in 20 mM phosphate buffer (pH 7.2) were mixed with increasing volumes of 8 M GdnHCl (molecular biology reagent grade; Sigma) prepared in 20 mM phosphate buffer (pH 7.2) so as to achieve a final protein concentration of 10 μM and the indicated final GdnHCl concentrations. Samples then were equilibrated at room temperature for 30 min prior to the recording of CD spectra.

RESULTS

Cloning of Mouse and Human MIF. We recently identified by N-terminal protein sequencing and cDNA cloning the mouse homolog of MIF among the proteins secreted by LPS-stimulated anterior pituitary cells (Bernhagen *et al.*, 1993). We now report the complete molecular cloning and the biochemical characterization of mouse MIF and human MIF obtained from the Jurkat H33HJ-JA1 T-cell line.

muMIF cDNA was prepared from the total RNA of LPS-stimulated anterior pituitary cells (AtT-20) and amplified with MIF primers as described previously (Bernhagen *et al.*, 1993). MIF cDNA then was cloned into the pT7Blue T-vector and subjected to DNA sequence analysis. The muMIF cDNA sequence obtained from six plasmid clones was compared to a previously published human T-cell MIF cDNA (Weiser *et al.*, 1989). Mouse MIF cDNA was found to display a 88.2% sequence homology to this huMIF sequence over a 348-nucleotide open reading frame and to be identical in sequence with recently reported mouse 3T3 fibroblast and mouse embryonic eye lens MIF cDNAs (Lanahan *et al.*, 1992; Wistow *et al.*, 1993; Bernhagen *et al.*, 1993) (EMBL Data Bank, accession number Z23048).

huMIF cDNA was prepared by RT/PCR of RNA isolated from resting Jurkat H33HJ-JA1 T-cells. MIF cDNA was amplified with flanking primers bearing *NdeI*/Ba*m*HI restriction sites, thus enabling us to subsequently clone the huMIF amplification product directly into a Nd*eI*/*Bam*HI-digested pET11b prokaryotic expression plasmid. The human MIF cDNA sequence then was obtained by sequencing both DNA strands of eight independently derived *E. coli* clones. This Jurkat T-cell MIF sequence was found to be identical to a recently reported human fetal lens MIF cDNA (Wistow *et al.*, 1993) and to a glycosylation inhibition factor (GIF) cDNA (Mikayama *et al.*, 1993) but differed from the first reported human T-cell MIF sequence obtained from the T-CEMB cell line (Weiser *et al.*, 1989) by a single base change at position 318. This G→A substitution produces a conservative Ser^{106}→Asn^{106} change in the deduced amino acid sequence and renders the human protein even more homologous with mouse MIF. Mouse pituitary MIF cDNA

```
                10        20        30        40        50        60
mu      MPMFIVNTNVPRASVPEGFLSELTQQLAQATGKPAQYIAVHVVPDQLMTFSGTNDPCALC
        :::::::::::::::::.:::::::::::::::::.:::::::::::::.:.:...:::::
hu      MPMFIVNTNVPRASVPDGFLSELTQQLAQATGKPPQYIAVHVVPDQLMAFGGSSEPCALC

                70        80        90       100       110
mu      SLHSIGKIGGAQNRNYSKLLCGLLSDRLHISPDRVYINYYDMNAANVGWNGSTFA
        :::::::::::::::.:::::::::..::.:::::::::::::::::::::::.::::
hu      SLHSIGKIGGAQNRSYSKLLCGLLAERLRISPDRVYINYYDMNAANVGWNNSTFA
```

FIGURE 1: Predicted amino acid sequence homology between mouse pituitary MIF and human Jurkat T-cell MIF. Potential N-linked glycosylation sites are underlined. mu: mouse MIF; hu: human MIF.

and human Jurkat cell cDNA exhibited 88.5% identity over a 348-nucleotide open reading frame, and the amino acid sequences deduced for mouse (AtT-20) and human (Jurkat) MIF were found to be 90% identical over the 115 amino acids (Figure 1). No apparent N-terminal signal sequences were evident in either the mouse or the human proteins. Two potential N-glycosylation sites were found at positions 75 and 110 of the muMIF amino acid sequence and at nearly identical positions in the human Jurkat MIF sequence (positions 73 and 110). Three cysteine residues (positions 57, 60, and 81) also were at identical places in the mouse and human MIF predicted amino acid sequences.

Expression and Purification of Recombinant MIF from E. coli. Recombinant muMIF and huMIF were expressed in *E. coli* by cloning mouse and human MIF cDNA into the IPTG-inducible pET expression plasmid system. Initial attempts to express mouse MIF from the pET15b vector, which creates an N-terminal oligo-histidine fusion protein and allows for facile purification of recombinant protein by ion metal affinity chromatography (IMAC) (Hoffmann & Roeder, 1991), were unsuccessful because MIF was resistant to the subsequent thrombin cleavage necessary to remove the oligo-histidine leader. Thus, we elected to express and then purify rmuMIF by conventional means and subcloned the muMIF cDNA into the plasmid pET11b. This produces a construct which bears a three-amino acid (Met-Asp-Ser) leader sequence attached to the N-terminus of MIF. huMIF also was expressed from the pET11b vector but was engineered by DNA amplification to begin at the second amino acid of the open reading frame, with the start methionine of MIF provided by the *Nde*I restriction site. The correct expression of MIF was verified by N-terminal amino acid sequencing of gel-purified protein (10 amino acids for muMIF), SDS-PAGE, and Western blotting with anti-AtT-20 MIF antibody (not shown). The pET11b-derived MIF was used for the subsequent purification of bioactive muMIF and huMIF.

Recombinant mouse or human MIF was found to constitute 40% of the total supernatant protein of *E. coli* lysates. Anion exchange chromatography at pH 7.5 resulted in approximately an 80% purification of mouse and human MIF (Figure 2, top). Subsequent application to a C8 reverse-phase column yielded pure protein for both the mouse and the human recombinant proteins, as verified by the appearance of single bands of predicted M_r (12.5 kDa) by SDS−PAGE/silver staining (Figure 2, top) and mass spectrometric analysis (described below). This simple and rapid two-step procedure enabled us to purify 1 mg of mouse or human MIF/50 mL of *E. coli* culture. After renaturation, 0.8−0.9 mg of soluble, bioactive recombinant MIF was obtained per 50 mL of culture. The overall yield of MIF protein from total bacterial supernatant protein was estimated to be 20%. This two-step purification method was elected for reasons of simplicity and rapidity and to minimize protein losses by nonspecific precipitation. Purification by C8 chromatography using a disposable, low-volume push column also served to remove the LPS carried over from *E. coli* host cells. Recombinant MIF purified by these procedures contained no more than trace amounts of LPS (4−8 ng of LPS/mg of MIF).

Purification of Native MIF. To assess more precisely the biological activities of recombinant MIF, we also purified native MIF from mouse tissue. Pituitary cells yielded insufficient quantities of MIF protein for biochemical characterization, and we established by Western blotting that the liver is an abundant source of MIF *in vivo* (Calandra *et al.*, 1994). We purified MIF from liver by a method similar to that used for recombinant MIF purification (Figure 2, middle). Mono Q anion exchange chromatography resulted in partial purification and increased the relative MIF content by approximately 25-fold. Subsequent application to the C8 push column afforded almost pure MIF. Upon SDS−PAGE/silver staining analysis however, five additional bands were detected that could not be removed by varying the elution conditions of the RP chromatography. A Pro S cation exchange chromatography step therefore was added prior to the C8 step to remove these contaminants. The purity and homogeneity of liver MIF was established by SDS−PAGE/silver staining (Figure 2, middle), Western blotting using anti-rmuMIF antibody (Figure 2, bottom), and mass spectrometric analysis. Laser desorption MS demonstrated a single protein species of M_r of 12 555 (described below). The MIF content of mouse liver acetone powder was estimated to be less than 0.1% of total protein, and we were able to reliably purify to homogeneity 50 μg at native liver MIF from 2 g of mouse liver powder.

Biochemical Characterization of MIF. The M_r for liver mouse MIF, rmuMIF, and rhuMIF were each between 12 000 and 13 000 as estimated by reducing SDS−PAGE (Figure 2, top and middle). We observed two potential N-linked glycosylation sites in the predicted amino acid sequence of mouse and human MIF and investigated the possibility that native muMIF is post-translationally glycosylated *in vivo*. Endoglycosidase F (PNGase F) digestion of purified liver MIF followed by reducing SDS−PAGE/Western blotting analysis showed no shift in the observed M_r (Figure 3), suggesting the absence of significant N-glycosylation of native liver MIF.

Gel exclusion chromatography of GdnHCl-denatured recombinant MIF showed a M_r of 14 256 and 13 803 for the mouse and human proteins, respectively, indicating that MIF elutes predominantly as a noncovalently associated monomer (Figure 4).

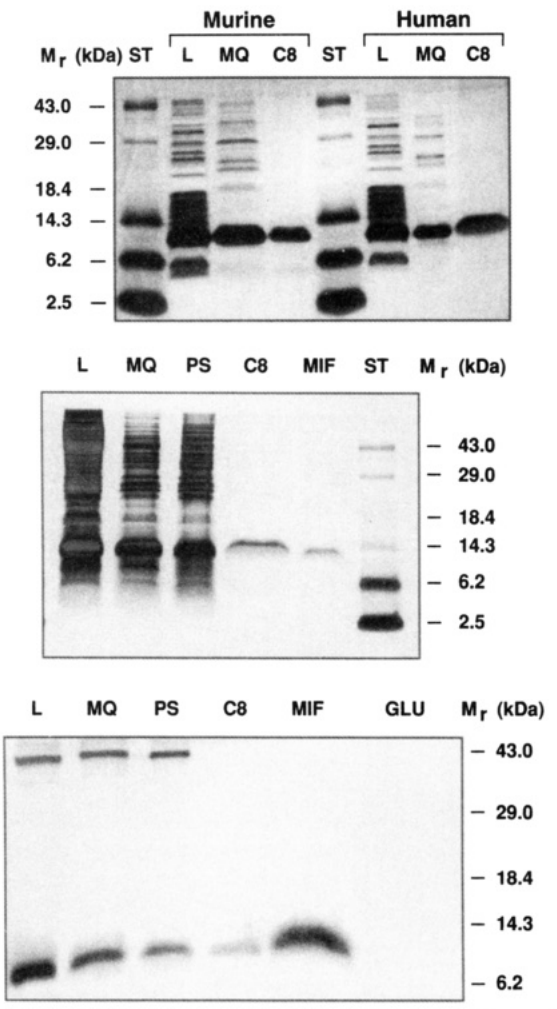

FIGURE 2: (top) Purification of recombinant mouse and human MIF as assessed by SDS−PAGE/silver staining analysis. Twenty-microliter aliquots were taken from MIF-containing fractions at each purification step, electrophoresed in 18% gels in the indicated lanes, and analyzed by silver staining. L = cleared bacterial lysate, MQ = Mono Q anion exchange chromatography, and C8 = C8 reverse-phase chromatography. Protein molecular weight markers (M_r) ranged from 2.5 to 43 kDa and were electrophoresed in the same gel in the indicated lanes (ST). (middle) Purification of native MIF from mouse liver as assessed by SDS−PAGE/silver staining analysis. Twenty-microliter aliquots were taken after each purification step, electrophoresed in 18% gels in the indicated lanes, and analyzed by silver staining. L = cleared cell lysate, MQ = Mono Q anion exchange chromatography, PS = Pro S cation exchange chromatography, and C8 = C8 reverse-phase chromatography. For comparison, 0.5 μg of rmuMIF (MIF) was analyzed in the same gel. Protein molecular weight markers (M_r) ranged from 2.5 to 43 kDa and were electrophoresed in the same gel in the indicated lane (ST). (bottom) SDS−PAGE/Western blotting analysis of purification of native MIF from mouse liver. Ten-microliter aliquots were taken after each purification step, electrophoresed in 18% gels in the indicated lanes, transferred to nitrocellulose membrane, and analyzed with anti-rmuMIF antibody. L = cleared cell lysate, MQ = Mono Q anion exchange chromatography, PS = Pro S cation exchange chromatography, and C8 and C8 reverse-phase chromatography. Elution of liver MIF after chromatography on glutathione affinity matrix (GLU)−30 ng of rmuMIF (MIF) was electrophoresed and transferred as a standard. Protein molecular weight markers (M_r) ranged from 6.2 to 43 kDa and were electrophoresed and transferred in the same gel in the indicated lane (ST).

We performed laser desorption MS of MIF to further assess glycosylation as well as the presence of any other significant post-translational modifications of MIF. Native MIF obtained from mouse liver was determined to have a

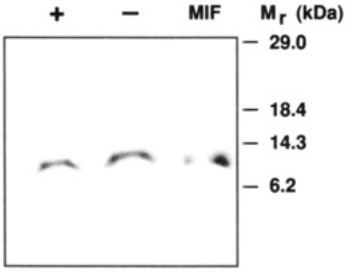

FIGURE 3: SDS−PAGE/Western blotting analysis of purified PNGase F-digested liver MIF. Purified liver MIF (100 ng) was incubated with PNGase F (+) or control buffer (−), electrophoresed in 18% gels, transferred to nitrocellulose membrane, and analyzed with anti-rmuMIF antibody. Endoglycosidase activity was confirmed by PNGase F digestion of IgG (not shown). rmuMIF (MIF) (30 ng) was electrophoresed and transferred as a standard. Protein molecular weight markers (M_r) ranged from 6.2 to 29 kDa and were electrophoresed and transferred in the same gel.

M_r of 12 555 (predicted MH^+ average mass of oxidized muMIF = 12 503). By comparison, rmuMIF (which bears a three-amino acid N-terminal leader sequence) was found to have a M_r of 12 814 (predicted MH^+ average mass of oxidized rmuMIF = 12 837). Ion-spray MS of rmuMIF yielded a similar mass (M_r = 12 804). Using laser desorption MS, rhuMIF was found to have a M_r of 12 521 (predicted MH^+ average mass of oxidized rhuMIF = 12 475). Differences observed between the experimental and theoretical predicted masses were within the margin of experimental error (0.1−1%) for these analyses. These data essentially rule out the presence of significant post-translational modifications of either native or recombinant MIF protein.

A 12 kDa protein purified from rat liver bearing N-terminal homology with huMIF has been reported to bind to glutathione affinity matrix and to exhibit glutathione-*S*-transferase (GST) activity (Blocki *et al.*, 1992). We were unable to demonstrate specific absorption of either liver MIF (Figure 2, bottom) or rmuMIF (not shown) to glutathione matrix. Furthermore, purified rmuMIF at a concentration of 20 μg/mL did not exhibit GST activity when assayed by standard methods using EPNP as the substrate (Fjellstedt *et al.*, 1973). Crude bacterial lysate supernatants containing approximately 50 μg/mL rmuMIF also did not show any detectable GST activity.

Bioactivity Profile. Purified rmuMIF displayed significant migration inhibitory activity when tested on human peripheral blood monocytes (Figure 5). A bell-shaped dose−response curve was observed with peak activity occurring at 0.1 μg/mL. The precise basis for diminished inhibitory activity at high MIF concentrations is not known, but similar dose−response profiles have been observed for chemotactic cytokines (Sherry *et al.*, 1992).

Previous studies have implicated MIF in the secretion of TNF-α (Calandra *et al.*, 1994) and NO (Herriott *et al.*, 1993) by macrophages. We tested the ability of recombinant MIF to induce TNF-α release by the mouse RAW 264.7 macrophage cell line. Both rmuMIF and rhuMIF added at concentrations of 0.1−10 μg/mL caused the release of bioactive TNF-α in the nanogram per milliliter range (Table 1). Despite species difference, rhuMIF at 1 μg/mL was found to be slightly more active than rmuMIF on mouse macrophages. At the same concentration (1 μg/mL), the TNF-α-inducing activity of MIF obtained from mouse liver was found to be higher than the activity of rmuMIF. When

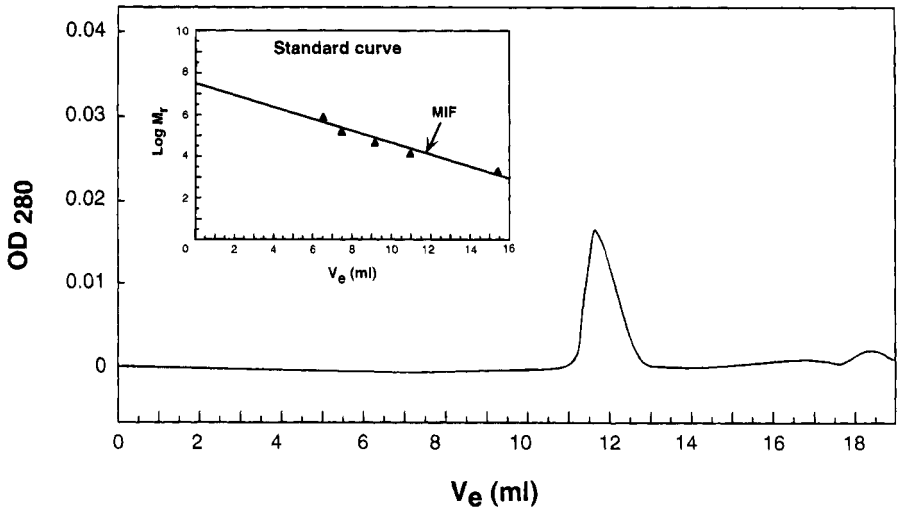

FIGURE 4: Gel exclusion chromatography of recombinant MIF. rhuMIF (40 μg), dissolved in 20 mM phosphate buffer (pH 7.2) containing 7 M GdnHCl, was chromatographed over a Superose 12 HR 10/30 column equilibrated with the same buffer. Eluted protein was detected by OD_{280} which is plotted with respect to elution volume (V_e). The elution position of the molecular weight standards is depicted in the inset as a plot of the logarithm of the molecular weight (log M_r) versus the elution volume (V_e). Molecular weight standards ranged from 1.35 to 670 kDa and were chromatographed under the same conditions as MIF. Gel chromatography of rmuMIF produced an essentially identical elution profile (not shown).

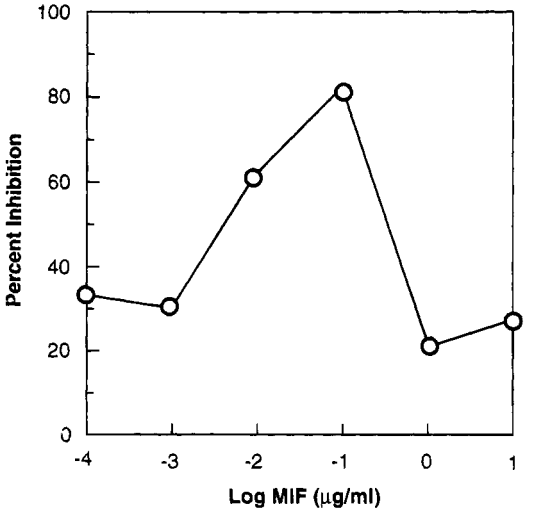

FIGURE 5: Inhibition of monocyte migration by recombinant MIF. The effect of various concentrations (0.0001−10 μg/mL) of rmuMIF on peripheral human blood monocyte migration was quantitated in a modified Boyden chamber. The percent of migration inhibition relative to buffer controls is plotted versus the logarithm of MIF concentration. Each point depicts the mean of independently performed duplicate determinations.

Table 1: MIF-Induced Secretion of TNF-α by Mouse Macrophages[a]

MIF (μg/mL)	secretion of TNF-α (ng/mL) induced by rmuMIF	rhuMIF	native MIF
10	ND	3.9 ± 2.8	ND
1	1.2 ± 0.1	3.4 ± 2.8	6.9 ± 3.4
0.1	0.2 ± 0.3	2.9 ± 2.4	0.2 ± 0.1
0.01	0	ND	0

[a] RAW 264.7 macrophages were prepared and incubated with MIF for 12−14 h as described in Experimental Procedures. After the incubations, macrophage culture supernatants were removed and analyzed by the L929 cell toxicity assay for TNF-α activity. TNF-α measurements were performed in duplicate, and TNF-α activity is expressed as the difference between the level produced by MIF-stimulated cells and that produced by nonstimulated control cells. Data are the mean ± SEM of at least three separate experiments. ND: not determined.

tested at a concentration of 0.1 μg/mL however, the TNF-α-inducing activity of mouse liver MIF was identical to rmuMIF. Similar findings were obtained when thioglycollate-elicited mouse peritoneal macrophages were used to study MIF-induced TNF-α release (not shown). Overall, the activity of native MIF was within the range observed for the recombinant proteins.

Native and recombinant MIF also induced NO production in macrophages (Table 2). However, significant MIF-induced NO production was observed only when macrophages were incubated with IFN-γ prior to stimulation with MIF. In RAW 264.7 macrophages, the activity of rhuMIF at 1 μg/mL was found to be approximately 4-fold higher than that of rmuMIF. Native MIF obtained from mouse liver also was more active in this assay than rmuMIF. MuMIF stimulated NO production from IFN-γ-primed, thioglycollate-elicited peritoneal exudate macrophages at levels which were comparable with those observed in RAW 264.7 cells. However, liver MIF at 1 μg/mL was not found to be more active than rmuMIF on this macrophage cell type.

The synthesis of NO by macrophages is induced by ≥10 ng/mL LPS, and this effect is potentiated by IFN-γ priming (Ding *et al.*, 1988; Lowenstein *et al.*, 1993). To exclude the possibility that the trace amounts of LPS present in recombinant MIF preparations contribute to NO production, we tested for MIF-induced NO release after neutralization of LPS with a large excess of polymyxin B. The production of NO was not reduced by polymyxin B treatment, arguing against a potentiating role for LPS in the stimulation of macrophages by MIF. In further control studies, the addition of neutralizing anti-rmuMIF antiserum (20 μL/mL) inhibited rmuMIF (1 and 10 μg/mL)-induced NO production, further confirming the specificity of macrophage stimulation by recombinant MIF (now shown).

Conformational and Structural Stability Analyses. Far-UV CD has been used widely to analyze the solution conformation of proteins and to verify native and renatured protein structures (Greenfield & Fasman, 1969). We performed far-UV CD spectroscopy and GdnHCl-induced

Table 2: NO Production in Mouse Macrophages Induced by MIF, Alone or in Combination with IFN-γ[a]

MIF (μg/mL)	formation of nitrite (μM) induced by rmuMIF	rhuMIF	native MIF
	− IFN-γ		
10[a]	0.2 ± 0.2	3.7 ± 2.1	ND
1[a]	0.5 ± 0.5	1.5 ± 1.0	0
0.1[a]	0.3 ± 0.3	0	0
0.01[a]	0	ND	0
	+ IFN-γ		
10[a]	12.3 ± 2.5	25.3 ± 7.5	ND
1[a]	5.7 ± 1.3	20.4 ± 5.7	9.8 ± 1.3
0.1[a]	1.7 ± 0.7	8.4 ± 2.6	3.1 ± 1.0
0.01[a]	1.9 ± 1.2	ND	0.5 ± 0.2
1[b]	12.5	ND	3.5

[a] RAW 264.7 macrophages were prepared and incubated with MIF for 12−14 h as described in Experimental Procedures. At the end of the incubation, 300 μL of culture supernatant was removed and mixed with 600 μL of Griess reagent and the concentration of nitrite measured. Nitrite measurements were performed in duplicate, and nitrite production is expressed as the difference between the level produced by MIF-stimulated cells versus nonstimulated or IFN-γ-treated control cells. Data are the mean ± SEM of at least three separate experiments. ND: not determined. [b] NO production by MIF-stimulated thioglycollate-elicited peritoneal macrophages in place of RAW 264.7 macrophages. Data are the mean of two separate experiments.

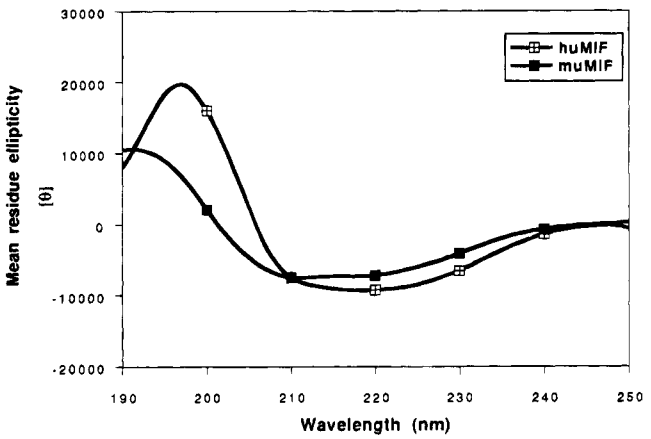

FIGURE 6: Far-UV CD spectrum of recombinant MIF. CD spectra of renatured rmuMIF and rhuMIF solutions were recorded at a concentration of 10 μM in 20 mM phosphate buffer (pH 7.2). The mean molar ellipticity per residue ([θ]) is plotted versus the wavelength.

unfolding studies with recombinant MIF to begin to assess the secondary structure and the structural stability of this protein in a solution environment. A representative far-UV CD spectrum (190-250 nm) of purified, renatured rmuMIF and rhuMIF at a concentration of 10 μM is shown in Figure 6. No concentration-dependent changes in the CD spectra of MIF were observed within the range studied (1.6−16 μM MIF). The spectrum for rmuMIF showed a pronounced positive ellipticity at 192 nm, a broad negative ellipticity between 209 and 222 nm, and small distinct minima at 210 and 222 nm. These data are consistent with a highly ordered secondary structure containing predominantly β-sheet but also α-helix conformation. The spectrum for rhuMIF showed a prominent positive ellipticity at 197 nm, and a strong negative ellipticity between 211 and 225 nm was observed. This CD spectrum also was consistent with a highly ordered secondary structure but was suggestive of a higher β-sheet content and a lower α-helix content than rmuMIF. Secondary structure compositions for both proteins

Table 3: Quantitative Analysis of the Secondary Structure Contents of Mouse and Human MIF[a]

method	secondary structure content (%) CD analyses 1[b]	2[c]	3[d]	4[e]	primary sequence predictions CF	GOR
	Mouse					
α-helix	15	16	NA	17 (13)[1]	11	8
β-sheet	42	39	NA	ND	36	39
unordered	35	36	NA	42 (31)[2]	32	33
β-turn	7	9	NA	ND	21	20
aromatic and disulfide	ND	ND	ND	− (26)[3]	ND	ND
parallel β-sheet/β-turn	ND	ND	ND	13 (9)[4]	ND	ND
antiparallel β-sheet	ND	ND	ND	29 (21)[5]	ND	ND
	Human					
α-helix	0	12	31	17 (14)[1]	30	19
β-sheet	73	55	39	ND	26	24
unordered	17	18	5	7 (6)[2]	27	32
β-turn	8	16	25	ND	17	25
aromatic and disulfide	ND	ND	ND	− (16)[3]	ND	ND
parallel β-sheet/β-turn	ND	ND	ND	32 (27)[4]	ND	ND
antiparallel β-sheet	ND	ND	ND	44 (37)[5]	ND	ND

[a] CD spectra of mouse and human MIF were measured at a concentration of 10 μM protein in 20 mM phosphate buffer (pH 7.2). Quantitative analysis of the CD spectra was performed by linear combination of the protein-derived basis sets/standard protein spectra according to various methods. Secondary structure contents were also calculated by predictions from the primary amino acid sequences using the methods of Chou and Fasman (1978) and Garnier, Osguthorpe, and Robson (1978). [b] Calculation by the Aviv Associates software system based on the unconstrained method of analysis of Brahms and Brahms (1980). [c] Calculation by the Lincomb program (Perczel *et al.*, 1992) based on the constrained method of analysis of Brahms and Brahms (1980). [d] Calculation by the Lincomb program using the standard spectra data set of Yang *et al.* (1974). [e] Calculation by the Lincomb program using the protein-derived basis set of Perczel, Park, and Fasman (1992). Values in parentheses[x] are the secondary structure components 1−5 of the basis set. The secondary structure contents (%) were calculated from these components as 100 times the basis weight of each component divided by the sum of the basis weights for the secondary structure components 1 + 2 + 4 + 5. CF: secondary structure predictions derived from the primary amino acid sequences by Chou and Fasman (1978). GOR: secondary structure predictions derived from the primary amino acid sequences by Garnier, Osguthorpe, and Robson (1978). ND: not determined by this method. NA: no allowed curve fit obtained.

then were estimated from computational fits of the CD spectra over the 190−250 nm range using the method of Brahms and Brahms (1980), which is frequently employed for the analysis of β-sheet-rich proteins. For comparison, the CD data were also subjected to computational fits using the method of Yang *et al.* (1974) and Perczel, Park, and Fasman (1992). Fasman's method also estimates the impact on the CD of aromatic amino acids and disulfide bonds and distinguishes between parallel and antiparallel β-sheets. The secondary structure contents calculated by these methods together with the secondary structure predictions derived from the primary amino acid sequence data are summarized in Table 3. Recombinant muMIF was found to exhibit a high β-sheet content which, depending on the method employed, varied from 39% to 42%. The α-helix, β-turn, and random coil fractions were determined to be 15%−17%, 7%−9%, and 35%−42%, respectively. The secondary structure component accounted for by aromatic amino acids and disulfide was estimated to be 26%. Recombinant huMIF contained a somewhat greater ordered structure, with a β-sheet content ranging from 39% to 73% and α-helix,

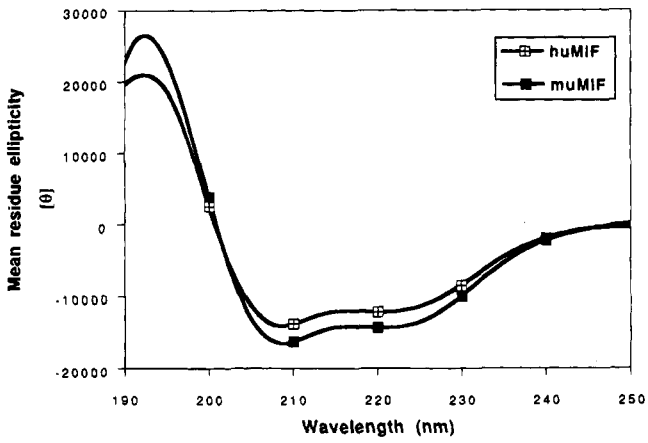

FIGURE 7: Effect of TFE on MIF conformation. CD spectra of renatured rmuMIF and rhuMIF were recorded with 50% TFE. MIF at a concentration of 10 μM was dissolved in 20 mM phosphate buffer (pH 7.2) containing 50% TFE 30 min before recording of the CD spectra. The mean molar ellipticity per residue ([θ]) is plotted versus the wavelength.

β-turn, and random coil conformations of 0%−31%, 8%−25%, and 5%−18%, respectively. The aromatic/disulfide component for huMIF was 16%. The CD data, together with the secondary structure predictions according to the Chou/Fasman and Garnier/Osguthorpe/Robson calculations, indicate that both recombinant mouse and human MIF contain a high fraction of β-sheet conformation. The spectroscopic data and the primary sequence predictions showed a similar low α-helical content for rmuMIF. Although the secondary structures predicted by Chou/Fasman and Garnier/Osguthorpe/Robson calculations suggest that there is a significant α-helical content in huMIF, the CD analyses suggest a low content of α-helical elements in rhuMIF.

Helical conformations induced at the membrane−water interface have been suggested to be important for ligand membrane interactions and to influence the binding of ligands to receptors (Kaiser & Kezdy, 1983; Fry *et al.*, 1992; Erne *et al.*, 1985). 2,2,2-Trifluoroethanol (TFE) induces and stabilizes the helical conformation of proteins with a helix-forming propensity and has been used to mimic the influence of membranes on polypeptide conformation (Sönnichsen *et al.*, 1992). To begin to test whether the α-helical content of either mouse or human MIF might be increased in the membranous environment, we performed far-UV CD analysis of rmuMIF and rhuMIF in 50% TFE. TFE significantly increased the α-helical content of rmuMIF, as demonstrated by a larger positive ellipticity at 192 nm and pronounced negative ellipticities at 208 and 222 nm (Figure 7). The calculated fraction of α-helix conformation (fit from Figure 7 by the various methods) increased from 15%−17% to 25%−39% in the presence of TFE. Recombinant huMIF, which also was found to have a low α-helical content in aqueous solution, also showed a significant content of α-helix in the presence of TFE as evident by a shift of the positive ellipticity from 197 to 192 nm and distinct negative ellipticities at 208 and 222 nm (Figure 7). Computational analysis of the spectroscopic data showed that the percentage of α-helix increased to 28%−47%. These data indicate that both mouse and human MIF are likely to adopt significant α-helical conformation in a membranous environment.

Protein structural stability can be quantitated by determining the free energy of unfolding, $\Delta G_{N\text{-}U}$, where N is the fraction of protein in the native state and U is the fraction in the unfolded state. One method used frequently to assess protein stability is to measure protein mean molar ellipticity per residue as a function of wavelength and GdnHCl concentration (Tanford, 1970; Greene & Pace, 1974; Pace, 1975). Unfolding curves expressed as the percentage of unfolded protein relative to native protein (i.e., the change in ellipticity at 222 nm) over the concentration of GdnHCl provide two measures of structural stability: (1) the midpoint of unfolding, $[\text{GdnHCl}]_{0.5}$, which can be deduced from the linear part of the unfolding curve (Pace, 1975) and (2) the free energy of unfolding at zero denaturant concentration, $\Delta G^\circ_{N\text{-}U}$, which can be extrapolated from the unfolding curve by the linear extrapolation method (LEM) (Pace, 1986; Schellmann, 1987; Santoro & Bolen, 1992). Both measures are based on the premise that unfolding follows a reversible two-state mechanism and that unfolding free energy is linearly dependent on denaturant concentration (Greene & Pace, 1974).

The CD spectra of rmuMIF were recorded between the wavelengths 210 and 250 nm in the presence of increasing concentrations of GdnHCl (0−7 M) (not shown). Recording below 210 nm was not performed due to strong scattering effects at these wavelengths. The MIF spectrum, defined in the absence of GdnHCl, changed visibly when >1.5 M GdnHCl was present, indicating a significant loss of conformational integrity. The featureless spectrum for fully denatured MIF in the presence of 7 M GdnHCl was similar to spectra observed for other fully unfolded proteins (Greenfield & Fasman, 1969). For quantitation of GdnHCl-induced unfolding, the unfolding of MIF α-helical structures was plotted by expressing the relative change in [θ] at 222 nm (percent unfolded) with respect to increasing concentrations of GdnHCl (Figure 8, top). The midpoint of unfolding was observed to be at 1.8 M GdnHCl. Next, the LEM was applied to extrapolate $\Delta G^\circ_{N\text{-}U}$ from a plot of $\Delta G_{N\text{-}U}$ versus the concentration of GdnHCl ([GdnHCl]). Data points of the linear portion of the curve in Figure 8, top, were replotted in Figure 8, bottom, according to the following equation:

$$\Delta G_{N\text{-}U} = \Delta G^\circ_{N\text{-}U} - m[\text{GdnHCl}]$$

where m is the slope of the curve, and subjected to linear regression analysis. Mouse MIF thus was calculated to have a $\Delta G^\circ_{N\text{-}U}$ of 11.75 kJ/mol. By comparison, globular proteins generally exhibit $\Delta G^\circ_{N\text{-}U}$ values of approximately 50 ± 15 kJ/mol (Pace 1990a,b; Tanford, 1970).

DISCUSSION

Macrophage migration inhibitory activity was identified almost 30 years ago as one of the first immunoregulatory activities to be mediated by a soluble factor (Bloom & Bennett, 1966; David, 1966). Over the years, several macrophage-activating properties (Nathan *et al.*, 1971, 1973; Chruchill *et al.*, 1975; Pozzi & Weiser, 1992) were associated with MIF activity which was believed to be a protein elaborated by lectin-activated T-lymphocytes (Weiser *et al.*, 1981). Nevertheless, elucidation of the distinct biochemical and biological properties of MIF has been imprecise. Many studies were performed with lymphocyte-conditioned medium which was subsequently shown to contain numerous cytokines (McInnes & Rennick, 1988; Thurman *et al.*, 1985), and despite the recent cloning of a human MIF (Weiser *et*

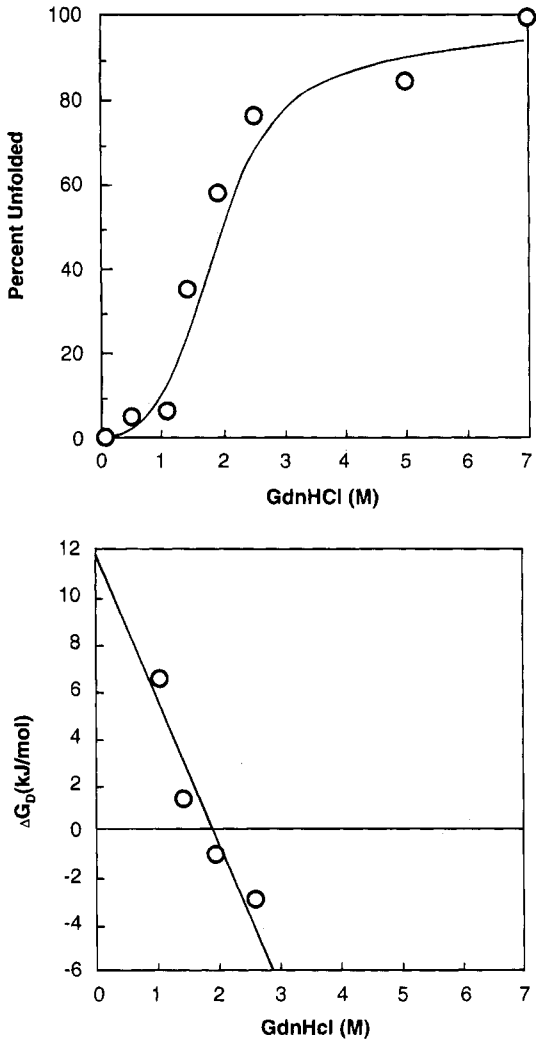

FIGURE 8: (top) GdnHCl-induced unfolding of rmuMIF. Unfolding was followed by the change in the mean molar ellipticity per residue [θ] at 222 nm (percent unfolded) and is plotted versus the concentration of GdnHCl. rmuMIF (10 μM) was studied in a solution of 20 mM phosphate buffer (pH 7.2) containing increasing concentrations of GdnHCl as indicated. (bottom) Change in unfolding free energy ($\Delta G_{N\text{-}U}$) as a function of GdnHCl concentration. The $\Delta G_{N\text{-}U}$ values were calculated from the top panel and replotted versus the GdnHCl concentration as shown. Data points were fit by linear least-squares analysis. $\Delta G°_{N\text{-}U}$ was obtained from the y-intercept calculated by the linear extrapolation method.

al., 1989), quantities of purified MIF sufficient for biochemical and biological studies have not been available.

We recently identified MIF to be a pituitary hormone that is released during endotoxemia and showed that anti-MIF antibody increased survival in a mouse model of endotoxic shock (Bernhagen *et al.*, 1993). We also have shown that the macrophage contains large quantities of stored, preformed MIF that is released by LPS stimulation (Calandra *et al.*, 1994). In the present report, we describe in full detail the molecular cloning of mouse and human MIF and the preparation of purified, bioactive MIF from both native and recombinant sources and provide the first characterization of a number of the biochemical and biological properties of this cytokine.

We cloned MIF from the AtT-20 mouse pituitary cell line and human MIF from the Jurkat T-cell line. Sequence analysis of mouse pituitary MIF and human T-cell MIF cDNA demonstrated a 90% homology between the mouse and human proteins. Cloned Jurkat T-cell MIF cDNA differs by one nucleotide from the published human T-cell MIF cDNA sequence which was obtained from the T-CEMB cell line (Weiser *et al.*, 1989) but is in agreement with a human MIF cDNA derived from human lens tissue (Wistow *et al.*, 1993) and with a T-cell glycosylation inhibitor factor (GIF) cDNA (Mikayama *et al.*, 1993). This single nucleotide difference results in a change in the deduced amino acid sequence ($Ser^{106}\rightarrow Asn^{106}$) which makes huMIF more homologous with the mouse protein.

DNA homology analysis showed that both mouse and human MIF lack a conventional N-terminal leader sequence. MIF thus joins a growing list of cytokines, such as interleukin-1 (Rubartelli *et al.*, 1990), basic fibroblast growth factor (bFGF) (Jackson *et al.*, 1992), and a secreted form of cyclophilin (Sherry *et al.*, 1992), which are released from cells by nonclassical protein secretion pathways.

As expected from their high amino acid sequence homology, mouse and human recombinant MIF behaved similarly in an *E. coli* expression system and were readily purified in high yield. Recombinant muMIF exhibited a higher tendency toward spontaneous aggregation. Whether this property is due to differences in the primary amino acid sequence between mouse and human MIF or to the presence in the muMIF expression of three additional amino acids at the N-terminus is unknown. Nevertheless, both proteins could be purified in milligram quantities by a simple two-step chromatographic procedure which additionally served to eliminate trace amounts of contaminating LPS.

The liver is an abundant souce of MIF *in vivo* (Calandra *et al.*, 1994), and we also purified native MIF from mouse liver by sequential anion and cation exchange followed by reverse-phase chromatography. Although a 12 kDa protein bearing N-terminal homology with huMIF has been isolated from rat liver by glutathione affinity chromatography (Blocki *et al.*, 1992), neither rmuMIF nor the mouse liver MIF we isolated was retained by glutathione affinity matrix under stringent conditions. Purified rmuMIF also did not exhibit any measurable GST activity (Blocki *et al.*, 1992).

Mouse and human MIF are both monomeric proteins with a M_r of approximately 12 500, a mass which is consistent with that predicted from the deduced amino acid sequences. The mass of native muMIF determined by laser MS was only slightly higher (and within experimental error) than the theoretical, predicted mass of muMIF, thus ruling out any significant post-translational modification of the native protein.

To achieve maximal bioactivity of recombinant MIF, we performed controlled dialysis of reduced, urea-denatured proteins. Recombinant muMIF caused a dose-dependent inhibition of monocyte migration. This effect was diminished at high MIF concentrations. Although the cellular mechanism responsible for this bell-shaped dose–response curve is unknown, similar activity profiles have been observed in other cytokine/monocyte migration systems (Sherry *et al.*, 1992). Both recombinant and native MIF were found to induce the release of significant quantities of TNF-α from mouse macrophages. MIF also promoted the macrophage release of NO, but significant MIF-induced NO production was observed only when macrophages were primed first with IFN-γ. This result differs from that of a recent report showing that MIF alone is sufficient to induce NO production by macrophages (Cunha *et al.*, 1993).

Whether this property was specific to the MIF-containing crude COS cell supernatants used in these experiments remains to be established. Nevertheless, the present studies are consistent with the potentiating effect of IFN-γ on macrophage NO production described previously (Ding *et al.*, 1988; Xie *et al.*, 1993). Taken together, these data verify the bioactivity of recombinant MIF prepared from *E. coli* and are consistent with the proinflammatory role of MIF in endotoxic shock (Bernhagen *et al.*, 1993).

To begin to obtain information about the three-dimensional structural properties of MIF, we performed CD spectroscopy together with GdnHCl-induced unfolding studies. CD spectroscopy is a valuable technique for obtaining protein conformational information in solution and has been used widely to study the inherent structural and thermodynamic stability of proteins. Secondary structure compositions predicted by CD spectroscopy frequently are in agreement with the protein structures subsequently obtained by X-ray crystallography (Greenfield & Fasman, 1969). Renatured recombinant MIF showed a high degree of conformational integrity when analyzed by CD spectroscopy and secondary structure content calculations. Recombinant muMIF was found to contain a high content of β-sheet conformation (39%−42%). Recombinant huMIF displayed an even higher fraction of β-sheet (39%−73%). Analysis of the CD data using the protein-derived basis set by Perczel, Park, and Fasman suggests that this difference in β-sheet content may be due to a significantly higher percentage of both parallel and antiparallel β-sheet components in the human homolog (27% and 37% versus 9% and 21%). Both proteins were found to exhibit a low content of α-helix conformation (approximately 15%). The method by Perczel, Park, and Fasman predicted an aromatic/disulfide component for both muMIF and huMIF (26% and 16%, respectively). Of note, both mouse and human MIF contain several aromatic residues as well as three cysteines, two of which are in close proximity to each other. A significant unordered secondary structure component, i.e., random coil conformation, was calculated for muMIF (35%−42%) but was found to be lower in huMIF (5%−18%). Given the high degree of primary sequence homology between the two proteins, it seems surprising that the CD spectra and the calculated secondary structure contents are significantly different between the mouse and human recombinant proteins. Whether these differences are due to the unique N-terminal structure of rmuMIF, which contains a three-amino acid leader sequence, is unclear. If so, it would point to an important role for the N-terminal domain in affecting the solution conformation of MIF. Alternatively, the observed conformational differences may be due to minor primary sequence differences between the mouse and human proteins. It is known that closely homologous polypeptide chains may assume markedly different three-dimensional structures depending on the precise local and nonlocal through-space interactions (Jaenicke, 1991). The structural information obtained by CD spectroscopy agreed only partially with secondary structure predictions determined by the algorithms of Garnier *et al.* (1978) and Chou and Fasman (1978).

TFE enhances the formation of α-helical structures and has been used experimentally to mimic the influence of membranes on polypeptide conformation and α-helix stabilization (Sönnichsen *et al.*, 1992). The addition of TFE to both recombinant mouse and human MIF induced a significant increase in the fraction of α-helix, suggesting that α-helical elements may play an important role both in MIF−cell membrane and MIF−receptor interactions (Kaiser & Kezdy, 1983; Fry *et al.*, 1992; Erne *et al.*, 1985).

The thermodynamic data derived from the GdnHCl-induced unfolding studies of rmuMIF ($[GdnHCl]_{0.5}$ = 1.8 M and $\Delta G°_{N\text{-}U}$ = 11.75 kJ/mol) indicate that MIF is of low to moderate structural stability compared with other globular proteins which have a similar $[GdnHCl]_{0.5}$ but a significantly higher $\Delta G°_{N\text{-}U}$ (50 ± 15 kJ/mol) than MIF (Pace, 1990a,b; Tanford, 1970). Experimental analysis of GdnHCl-induced unfolding is based on the premise of a two-state unfolding mechanism. With respect to MIF, the shape of the sigmoid curve, the value of the slope m (6.6 (kJ/mol)/M, Figure 8, bottom), and preliminary temperature-denaturation studies which show an isodichroic point are each consistent with a two-state equilibrium mechanism of unfolding (Greene & Pace, 1974; Pace, 1975, 1986). We currently are elucidating the precise positions of the disulfide linkages in MIF and analyzing the effects of these linkages on conformational stability. More complete structural information must await the ultimate solution of the three-dimensional structure of MIF by NMR spectroscopy and X-ray crystallography.

In conclusion, the present studies establish a high degree of structural and functional homology between MIF prepared from recombinant bacterial and eukaryotic tissue sources. The availability of large quantities of purified, bioactive MIF will greatly facilitate future investigation into the biological properties of this inflammatory mediator and newly described pituitary hormone. Ongoing structural and conformational studies also will assist in the ultimate development of pharmacological agents aimed at either inhibiting or promoting MIF activity in diverse pathophysiological conditions.

ACKNOWLEDGMENT

We are grateful to J. Fernandez and the Rockefeller University biopolymer facility for protein sequencing and to A. Kapurniotu, J. W. Taylor, and N. Greenfield for discussions and assistance with the CD spectroscopy. We thank N. Greenfield and G. D. Fasman for kindly providing the Lincomb program and G. Paulus (the Institut für Peptidforschung (Hannover, Germany), Shimadzu Europa GMBH), Y. Al-Abed, and S. Stoeva for the laser desorption MS analyses. We also thank J. Metzger and the Institut für Organische Chemie der Universität Tübingen for the ion-spray MS, B. Sherry for helpful discussions and assistance with the macrophage migration assay, and K. Manogue for reviewing the manuscript.

REFERENCES

Allen, G. (1981) in *Sequencing of Proteins and Peptides* (Work, T. S., Burdon, R. H., Eds.) Elsevier, Amsterdam, New York.

Anderson, N. L., Nance, S. L., Pearson, T. W., & Anderson, N. G. (1982) *Electrophoresis 3*, 135−142.

Bernhagen, J., Calandra, T., Mitchell, R. A., Martin, S. B., Tracey, K. J., Voelter, W., Manogue, K. R., Cerami, A., & Bucala, R. (1993) *Nature 365*, 756−759.

Blocki, F. A., Schlievert, P. M., & Wackett, L. P. (1992) *Nature 360*, 269−270.

Bloom, B., & Bennett, B. (1966) *Science 153*, 80−82.

Boyden, S. V. (1962) *J. Exp. Med. 115*, 453−466.

Bradford, M. (1976) *Anal. Biochem. 72*, 248−256.

Brahms, S., & Brahms, J. (1980) *J. Mol. Biol. 138*, 149−178.
Calandra, T., Bernhagen, J., Mitchell, R. A., & Bucala, R. (1994) *J. Exp. Med. 179*, 1895−1902.
Chou, P. Y., & Fasman, G. D. (1978) *Adv. Enzymol. 47*, 45−148.
Churchill, W. H., Piessens, W. F., Sulis, C. A., & David, J. R. (1975) *J. Immunol. 115*, 781−785.
Clark, J. M. (1988) *Nucleic Acids Res. 16*, 9677−9686.
Cunha, F. Q., Weiser, W. Y., David, J. R., Moss, D. W., Moncada, S., & Liew, F. Y. (1993) *J. Immunol. 150*, 1908−1912.
David, J. R. (1966) *Proc. Natl. Acad. Sci. U.S.A. 56*, 72−77.
David, J. R. (1993a) *J. Immunol. 151*, last page (unnumbered).
David, J. R. (1993b) *Proc. Natl. Acad. Sci. U.S.A. 90*, 12056.
Ding, A. H., Nathan, C. F., & Stuehr, D. J. (1988) *J. Immunol. 141*, 2407−2412.
Erne, D., Sargent, D. F., & Schwyzer, R. (1985) *Biochemistry 24*, 4263−4261.
Fjellstedt, T. A., Allen, R. H. Duncan, B. K. & Jakoby, W. B. (1973) *J. Biol. Chem. 248*, 3702−3707.
Fry, D. C., Madison, V. S., Greeley, D. N., Felix, A. M., Heimer, E. P., Frohman, L., Campbell, R. M., Mowles, T. F., Toome, V., & Wegrzynski, B. B. (1992) *Biopolymers 32*, 649−666.
Garnier, J., Osguthorpe, D. J., & Robson, B. (1978) *J. Mol. Biol. 120*, 97−120.
Greene, R. F., & Pace, C. N. (1974) *J. Biol. Chem. 249*, 5388−5393.
Greenfield, N., & Fasman, G. D. (1969) *Biochemistry 8*, 4108−4116.
Herriott, M. J., Jiang, H., Stewart, C. A., Fast, D. J., & Leu, R. W. (1993) *J. Immunol. 150*, 4524−2531.
Hillenkamp, F., & Karas, M. (1990) *Methods Enzymol. 193*, 280−295.
Hoffmann, A., & Roeder, R. G. (1991) *Nucleic Acids Res. 19*, 6337−6338.
Jackson, A., Friedman, S., Zhan, X., Engleka, K. A., Forough, R., Maciag, T. (1992) *Proc. Natl. Acad. Sci. U.S.A. 89*, 10691−10695.
Kaiser, E. T., & Kezdy, F. J. (1983) *Proc. Natl. Acad. Sci. U.S.A. 80*, 1137−1143.
Laemmli, U. K. (1970) *Nature 227*, 680−682.
Lanahan, A., Williams, J. B., Sanders, L. K., & Nathans, D. (1992) *Mol. Cell. Biol. 12*, 3919−3929.
Lowenstein, C. J., Alley, E., Raval, P., Snyder, S. H., Russel, S. W., & Murphy, W. (1993) *Proc. Natl. Acad. Sci. U.S.A. 90*, 9730−9734.
McInnes, A., & Rennick, D. M. (1988) *J. Exp. Med. 167*, 598−611.
Mikayama, T., Nakano, T., Gomi, H., Nakagawa, Y., Liu, Y.-C., Sato, M., Iwamatsu, A., Ishii, Y., Weiser, W. Y., & Ishizaka, K. (1993) *Proc. Natl. Acad. Sci. U.S.A. 90*, 10056−10060.
Nathan, C. F., Karnovsky, M. L., & David, J. R. (1971) *J. Exp. Med. 133*, 1356−1376.
Nathan, C. F., Remold, H. G., & David, J. R. (1973) *J. Exp. Med. 137*, 275−288.
Pace, C. N. (1975) *CRC Crit. Rev. Biochem. 3*, 1−43.
Pace, C. N. (1986) *Methods Enzymol. 131*, 266−280.
Pace, C. N. (1990a) *Trends Biochem. Sci. 15*, 14−17.
Pace, C. N. (1990b) *Trends Biotechnol. 8*, 93−98.
Perczel, A., Park, K., & Fasman, G. D. (1992) *Anal. Biochem. 203*, 83−93.
Poehling, H. M., & Neuhoff, V. (1981) *Electrophoresis 2*, 141−147.
Pozzi, L. M., & Weiser, W. Y. (1992) *Cell. Immunol. 145*, 372−375.
Rubartelli, A., Cozzolino, F., Talio, M., & Sitia, R. (1990) *EMBO J. 9*, 1503−1510.
Santoro, M. M., & Bolen, D. W. (1992) *Biochemistry 31*, 4901−4907.
Schellmann, J. A. (1987) *Biopolymers 26*, 549−559.
Sherry, B., Yarlett, N., Strupp, A., & Cerami, A. (1992) *Proc. Natl. Acad. Sci. U.S.A. 89*, 3511−3515.
Smith, D. B., & Johnson, K. S. (1988) *Gene 67*, 31−40.
Sönnichsen, F. D., Van Eyk, J. E., Hodges, R. S., & Sykes, B. D. (1992) *Biochemistry 31*, 8790−8798.
Studier, F. W., Rosenberg, A. H., Dunn, J. J., & Dubendorff, J. W. (1990) *Methods Enzymol. 185*, 60−89.
Stuehr, D. J., & Marletta, M. A. (1987) *Cancer Res. 47*, 5590−5594.
Tabor, S., & Richardson, C. C. (1987) *Proc. Natl. Acad. Sci. U.S.A. 84*, 4767−4771.
Tanford, C. (1970) *Adv. Protein Chem. 24*, 1−95.
Thurman, G. B., Braude, I. A., Gray, P. W., Oldham, R. K., & Stevenson, H. C. (1985) *J. Immunol. 134*, 305−309.
Weiser, W. Y., Greineder, D. K., Remold, H. G., & David, J. R. (1981) *J. Immunol. 126*, 1958−1962.
Weiser, W. Y., Temple, P. A., Witek-Gianotti, J. S., Remold, H. G., Clark, S. C., & David, J. R. (1989) *Proc. Natl. Acad. Sci. U.S.A. 86*, 7522−7526.
Wistow, G. J., Shaughnessy, M. P., Lee, D. C., Hodin, J., & Zelenka, P. S. (1993) *Proc. Natl. Acad. Sci. U.S.A. 90*, 1272−1275.
Wolpe, S. D., Davatelis, G., Sherry, B., Beutler, B., Hesse, D. G., Nguyen, H. T., Moldawer, L. L., Nathan, C. F., Lowry, S. F., & Cerami, A. (1988) *J. Exp. Med. 167*, 570−575.
Xie, Q., Whisnant, R., & Nathan, C. (1993) *J. Exp. Med. 177*, 1779−1784.
Yang, J. T., Wu, C. S., & Martinez, H. M. (1974) *Methods Enzymol. 130*, 208−269.